JOURNAL OF THERMOPHYSICS AND HEAT TRANSFER
Vol. 24, No. 4, October–December 2010

New In Situ Method for Estimating Thermal Diffusivity Using Rate-Based Temperature Sensors

J. I. Frankel,* M. Keyhani,† B. Elkins,‡ and R. V. Arimilli†
University of Tennessee, Knoxville, Tennessee 37996-2210

DOI: 10.2514/1.46300

This paper proposes an experimental methodology for estimating the thermal diffusivity α in a one-dimensional half-space geometry based on two in situ positioned probes that can acquire temperature and the first- and second-time derivatives of temperature. The thermal diffusivity is estimated at each sampled time by solving an nth-degree polynomial in the thermal diffusivity. The degree of the α polynomial and the required order of the time-derivative sensors depend on the chosen spatial truncation of the Taylor series. This approach does not require the specification of the imposed surface boundary condition. Additionally, a novel sensitivity analysis is proposed for guiding sensor placement that ensures a maximum, absolute sensitivity between the two probes, and it illustrates that a single point in time can be identified whereby the thermal diffusivity can be accurately approximated in an analogous manner to the determination of the time constant of a first-order system. Finally, the method is demonstrated with a numerical simulation.

Nomenclature

C	=	heat capacitance, kJ/(kg K)
d	=	sensor position ratio, x_2/x_1
Fo_j	=	Fourier modulus at fixed position, $\alpha t/x_j^2$, x_j ($j = 1, 2$)
$Fo_{2,\infty}$	=	Fourier modulus at spatial position x_2 at maximum absolute intersensitivity, $\alpha^* t^*/x_2^2$
k	=	thermal conductivity, W/(m K)
M	=	data sample size
q_o''	=	surface heat flux, W/m^2
q''	=	heat flux, W/m^2
T	=	temperature, °C
$\dot{T}$	=	sensor heating rate, °C/s
$\ddot{T}$	=	sensor second-time derivative of temperature, °C/s^2
T_o	=	initial condition, °C
T_{ref}	=	reference temperature, Eq. (7b), °C
t	=	time, s
$t_{p,2}$	=	estimated penetration time at $x = x_2$, s
t^*	=	estimated time for maximum absolute intersensitivity, s
u	=	dummy time variable, s
x	=	spatial coordinate, m
x_j	=	probe location, $j = 0, 1, 2, \ldots, m$
Z_α	=	sensitivity function, Eq. (4a), °C s/m^2
α	=	thermal diffusivity, m^2/s
α_{exact}	=	exact thermal diffusivity, m^2/s
α^*	=	estimated thermal diffusivity from intersensitivity analysis, m^2/s
γ_k	=	random number between $[-1, 1]$, $k = 1, 2, \ldots, M$, Eq. (12)
Δt	=	sampling time, s
ΔZ_α	=	intersensitivity function, Eq. (5a), °C s/m^2
$\Delta\Phi_\alpha$	=	modified intersensitivity function, Eq. (5b), °C
$\Delta\phi_\alpha$	=	dimensionless modified intersensitivity function, Eq. (7a)
$\|\Delta\phi_\alpha\|_\infty$	=	maximum dimensionless modified intersensitivity function
ε_T	=	noise factor for temperature data, Eq. (12)
$\varepsilon_{\dot{T}}$	=	noise factor for heating-rate data, Eq. (12)
$\varepsilon_{\ddot{T}}$	=	noise factor for second-time derivative of temperature data, Eq. (12)
ρ	=	density, kg/m^3
Φ_α	=	modified sensitivity function, Eq. (4b), °C

Presented as Paper 2009-4252 at the 41st Thermophysics Conference, San Antonio, TX, 22–25 June 2009; received 12 July 2009; revision received 17 July 2010; accepted for publication 18 July 2010. Copyright © 2010 by the American Institute of Aeronautics and Astronautics, Inc. All rights reserved. Copies of this paper may be made for personal or internal use, on condition that the copier pay the $10.00 per-copy fee to the Copyright Clearance Center, Inc., 222 Rosewood Drive, Danvers, MA 01923; include the code 0887-8722/10 and $10.00 in correspondence with the CCC.

*Professor, Mechanical, Aerospace, and Biomedical Engineering Department. Associate Fellow AIAA.

†Professor, Mechanical, Aerospace, and Biomedical Engineering Department.

‡Ph.D. Student, Aerospace and Biomedical Engineering Department. Student Member AIAA.

I. Introduction

THE accurate measurement of temperature, heat flux, and thermophysical properties are basic quantities of interest in heat transfer and aerothermodynamics. In many applications, these quantities must be deduced or resolved from inverse methods based on either function reconstruction or parameter estimation. This is a nontrivial task since the reconstitution process is normally ill posed. For example, in boundary condition reconstruction, interior temperature measurement errors are amplified in the projection process from the interior to the surface [1–4]. This process becomes worse as the sampling rate is increased. Thus, novel approaches are required for estimating the surface heat flux and temperature based on interior measurements.

As part of the journey to resolve such problems, a common thread has been identified for a stable reconstitution process involving either function reconstruction or parameter estimation. This thread involves the time derivative or time derivatives of temperature, and it requires careful interpretation and proper representation when used in the inversion process. Aerospace applications that can benefit from this observation include 1) in situ methods for estimating heat flux, 2) in situ methods for locating the onset of transition in hypersonic flows, and 3) in situ methods for estimating thermophysical properties involving both isotropic and anisotropic materials. This paper offers a novel concept for the in situ measurement of thermal diffusivity.

Section II presents motivation and background material germane to the present contribution by suggesting that rate-based measurements be pursued. Section III provides some recent sensor results indicating that it is possible to fabricate an accurate rate-based sensor using a voltage-rate interface that takes advantage of diffusion theory. Section IV describes the novel concept of intersensitivity analysis based on a multiprobe system. This analysis assists in establishing guidelines for sensor placement in the estimation of the

thermal diffusivity. Section V proposes a novel two-probe formulation for estimating thermal diffusivity in a simple geometry that uses higher time-derivative temperature sensors. Section VI presents simulation results indicating the merit of such an approach. Finally, Sec. VII provides some conclusions.

II. Motivation

To motivate the importance of a time-domain viewpoint to heat flux, which is a key ingredient to the proposed methodology, we present a synopsis of recent findings [1–4]. Before proceeding, let us elucidate the differences between spatial (or space domain) and temporal (or time domain) viewpoints on heat flux. The normal space domain viewpoint of heat flux is based on 1) using a constitutive relationship (Fourier's law) for estimating the heat flux q'', irrespective of steady-state or transient conditions and 2) using Fourier's law, as approximated by $q'' \approx -k\Delta T/\Delta x$, for heat flux gauge development.

An alternative viewpoint for investigating transient problems lies in the implementation of a time-domain analysis. A time-domain viewpoint of heat flux is based on combining the general law (conservation of energy) and constitutive relationship (Fourier's law) to form an integral relationship [1–4] between heat flux and temperature in the time variable.

The time-domain view explicitly exposes the ill-posed nature associated with recovering the heat flux by displaying the time rate of change of temperature, $\partial T/\partial t$ (°C/s).

Transient analysis is highly useful in arcjet and wind-tunnel investigations. For example, heat flux is often estimated in arcjet studies by using null-point calorimetry [5]. Null-point calorimetry involves designing the well geometry for the probe to match the surface temperature of the semi-infinite heat conduction problem. In general, the heat flux $q''(x,t)$ anywhere in the one-dimensional semi-infinite geometry can be acquired from the integral relationship [1–4]:

$$q''(x,t) = -\sqrt{\frac{\rho Ck}{4\pi}} \int_{u=0}^{t} \frac{T(x,u)}{(t-u)^{3/2}}\,\mathrm{d}u, \qquad x,t \geq 0 \tag{1a}$$

where $T(x,t)$ can be viewed as the measured temperature (assuming the sensor time constant is zero) at some point $x \geq 0$. Without loss of generality, the initial condition is assumed trivial; that is, $T_o = 0°\mathrm{C}$. Both null-point calorimetry [5] and thin film gauges [6,7] are often analyzed using a similar expression but evaluated at $x = 0$. Equation (1a) is actually the Hadamard equivalent [1] that involves finite-part integration of

$$q''(x,t) = \sqrt{\frac{\rho Ck}{\pi}} \int_{u=0}^{t} \frac{\partial T}{\partial u}(x,u)\,\frac{\mathrm{d}u}{\sqrt{t-u}}, \qquad x,t \geq 0 \tag{1b}$$

which indicates that temperature data are implicitly differentiated with respect to time since both expressions are equivalent under Hadamard finite-part integration, as they both originate from the identical heat equation. Reference [1] indicates that Eqs. (1a) and (1b) can be directly derived without resorting to the Hadamard interpretation. However, Hadamard finite-part integration is required to directly arrive at Eq. (1a) from Eq. (1b). Recasting Eq. (1b) as Eq. (1a) does not change the behavior of the inherent temperature measurement error. However, it has been shown that the problem statement is well posed if one could directly measure the heating rate $\partial T/\partial t$ without introducing numerical or analog differentiation. This leads to new analog and digital filtering strategies [1] that assure the proper representation of the heating rate. This mathematical fact, per Eq. (1b), has often been overlooked by the research community. Finally, it should be noted that Eq. (1a) can be expressed by the Volterra integral equation of the first kind [1,8] for heat flux as

$$T(x,t) = \frac{1}{\sqrt{\pi k\rho C}} \int_{u=0}^{t} \frac{q''(x,u)}{\sqrt{t-u}}\,\mathrm{d}u, \qquad x,t \geq 0 \tag{1c}$$

Equation (1c) indicates that stability issues will dominate in the reconstruction of the heat flux when provided with discrete, noisy temperature data, since first-kind Volterra integral equations are mildly ill posed [8]. Finally, the collection of thermophysical properties $\sqrt{k\rho C}$ is often called the coefficient of heat penetration or thermal effusivity.

Frankel [1] and Frankel et al. [2–4] have developed a unified and generalized system of multidimensional, semi-infinite heat flux-temperature integral relationships for isotropic, orthotropic, and anisotropic heat conduction, and they have investigated the effects of noise [9] in the measured data on the prediction of heat flux. Numerical differentiation [10,11] of noisy discrete data is known to be ill posed as the sampling rate is increased for fixed time domain.

III. Sensor Results

Recently, Frankel et al. [12], Elkins et al. [13], and Kruttiventi et al. [14] have developed two highly accurate sensors involving well-designed voltage-rate interfaces for estimating temperature T, the first-time derivative of temperature $\dot{T}$, and the second-time derivative of temperature $\ddot{T}$. Here, the dots above the temperature T represent time derivatives from a sensor. These sensors can be used for a variety of real-time studies including the estimation of heat flux, locating sudden changes in surface heat flux from an in-depth series of measurements, and thermal management.

IV. Intersensitivity Analysis

Before proceeding to develop new relationships for estimating thermal diffusivity, it appears beneficial to develop a sensitivity analysis for guiding the experimental design process. In this section, we offer a novel sensitivity analysis that offers significant insight into sensor placement. It is based on a new principle involving intersensitivity that is established between two thermocouples. The rationale and development of this concept is now discussed in the context of an idealized experimental setup. For demonstration purposes, we consider the mathematically convenient one-dimensional half-space geometry, as described in Fig. 1. The heat equation is given by

$$\frac{1}{\alpha}\frac{\partial T}{\partial t}(x,t) = \frac{\partial^2 T}{\partial x^2}(x,t), \qquad (x,t) \geq 0 \tag{2a}$$

subject to the idealized surface heat flux condition

$$q''(0,t) = q''_o, \qquad t > 0 \tag{2b}$$

and the uniform initial condition

$$T(x,0) = T_o = 0°\mathrm{C}, \qquad x \geq 0 \tag{2c}$$

From a Fourier cosine transform technique, we can obtain the analytic solution [1]

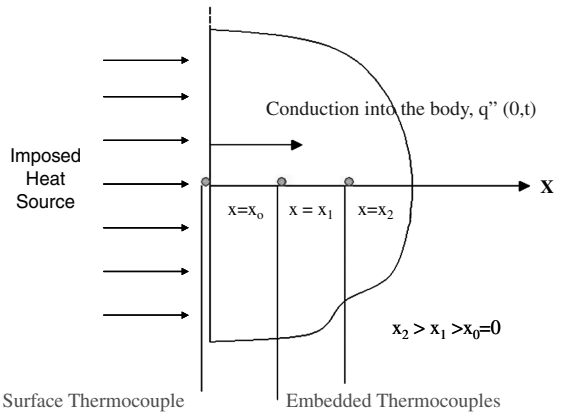

Fig. 1 Schematic of one-dimensional half space with sensors.

$$T(x,t) = \frac{1}{\sqrt{\rho C k \pi}} \int_{u=0}^{t} q''(0,u) \frac{e^{-\{x^2/[4\alpha(t-u)]\}}}{\sqrt{t-u}}\, du, \qquad (x,t) \geq 0 \tag{3a}$$

or explicitly upon using Eq. (2b), we obtain

$$T(x,t) = \frac{q_o''}{k}\sqrt{\frac{\alpha}{\pi}}\left[2\sqrt{t}e^{-(x^2/4\alpha t)} - x\sqrt{\frac{\pi}{\alpha}}erfc\left(\frac{x}{2\sqrt{\alpha t}}\right)\right] \qquad (x,t) \geq 0 \tag{3b}$$

The explicit nature of the solution permits a direct sensitivity analysis [15] to be performed. Let the sensitivity coefficient of interest for this investigation be defined as

$$Z_\alpha \triangleq \frac{\partial T}{\partial \alpha}(x,t;\alpha) = \frac{q_o''\sqrt{t}}{k\sqrt{\alpha\pi}} e^{-(x^2/4\alpha t)}, \qquad (x,t) \geq 0 \tag{4a}$$

and let the modified sensitivity coefficient [15] be defined as

$$\Phi_\alpha \triangleq \alpha Z_\alpha = \alpha \frac{\partial T}{\partial \alpha}(x,t;\alpha) = \frac{q_o''\sqrt{\alpha t}}{k\sqrt{\pi}} e^{-(x^2/4\alpha t)}, \qquad (x,t) \geq 0 \tag{4b}$$

Here, Z_α has units of $^\circ$C s/m^2, while Φ_α has units of $^\circ$C. For numerical demonstration purposes, let $q_o'' = 10^6$ W/m^2, $\alpha = 3.75 \times 10^{-6}$ m^2/s, and $k = 14.7$ W/(m K). These material properties are reminiscent of stainless steel while the heat flux can be imposed from a laser. Figures 2 and 3 display the temperature T and modified sensitivity function Φ_α at the three indicated locations. Observe that both functions display similar shapes and that Φ_α does not display a local absolute maximum. That is, the sensitivity analysis does not provide an optimal point in time from which we can extract the thermal diffusivity where the measurement errors least affect the estimated value of the thermal diffusivity. However, let us propose the following thought experiment involving two in-depth thermocouples. With this construction, a direct (well-posed) mathematical region exists between the two sensors (see Fig. 1, say x_1 and x_2). This arrangement does not require any knowledge of the imposed boundary condition at $x = 0$ in order to resolve the temperature distribution between x_1 and x_2, since the two temperature data streams define a region that is mathematically well posed (i.e., state estimation). This is an additional benefit to the proposed approach, as will be demonstrated in the next section.

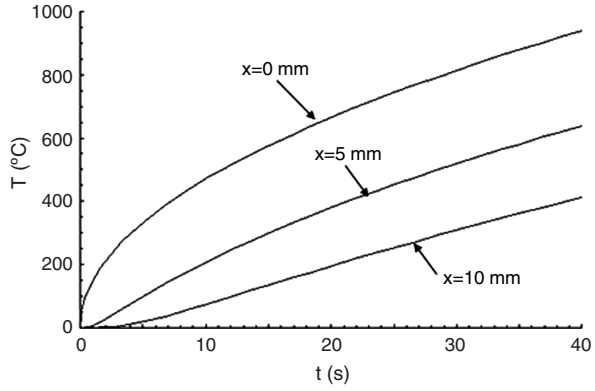

Fig. 2 Temperature histories at the three indicated positions.

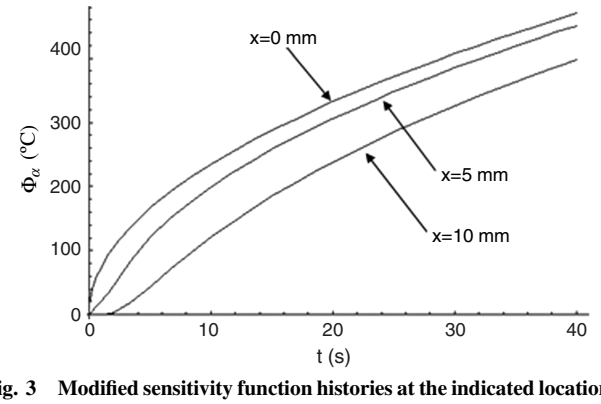

Fig. 3 Modified sensitivity function histories at the indicated locations.

The concept of intersensitivity is now developed based on the proposed thought experiment. The objective is to develop an analogous methodology for estimating the optimal placement of sensors that follows from the time constant of a first-order system. With this in mind, consider two thermocouple locations denoted as x_j and x_{j+1}, where $j = 0, 1, \cdots$ and $x_{j+1} > x_j$. Next, we define the intersensitivity and modified intersensitivity functions as

$$\Delta Z_\alpha \triangleq Z_\alpha(x_{j+1},t;\alpha) - Z_\alpha(x_j,t;\alpha) \tag{5a}$$

and

$$\Delta\Phi_\alpha \triangleq \alpha \Delta Z_\alpha \tag{5b}$$

respectively. Hence, we can explicitly express these functions as

$$\Delta Z_\alpha \triangleq \frac{\partial(\Delta T)}{\partial \alpha} = \frac{q_o''\sqrt{t}}{k\sqrt{\alpha\pi}}(e^{-(x_{j+1}^2/4\alpha t)} - e^{-(x_j^2/4\alpha t)}), \qquad t \geq 0 \tag{6a}$$

$$\Delta\Phi_\alpha \triangleq \alpha\Delta Z_\alpha = \alpha\frac{\partial(\Delta T)}{\partial \alpha} = \frac{q_o''\sqrt{\alpha t}}{k\sqrt{\pi}}(e^{-(x_{j+1}^2/4\alpha t)} - e^{-(x_j^2/4\alpha t)}) \qquad t \geq 0 \tag{6b}$$

For demonstration purposes, let $x_j = j\Delta x$, and $j = 0, 1, 2, 3, 4$, where $\Delta x = 5$ mm, and continue with the previously defined parameters.

Figure 4 displays a family of curves for $\Delta\Phi_\alpha$ over various sensor location pairings. This figure indicates that a family of absolute maximums results analogous to the thermocouple time constant example previously described. Thus, it appears possible to locate the maximum intersensitivities through analytical minimization of Eq. (6b).

Before proceeding further, let us express our system in dimensionless form for additional convenience and insight. Further, let us reduce the sensor location notation to only involve sensors 1 and 2, per Fig. 1, although they remain arbitrary in position.

Equation (6b) can be readily manipulated into the dimensionless form

$$\Delta\phi_\alpha \triangleq \frac{\Delta\Phi_\alpha}{T_{\text{ref}}} = \sqrt{Fo_2}(e^{-(1/4Fo_2)} - e^{-(1/4Fo_1)}) = \sqrt{Fo_2}(e^{-(1/4Fo_2)} - e^{-(1/4d^2Fo_2)}) \tag{7a}$$

where the reference temperature T_{ref} and the Fourier number are defined as

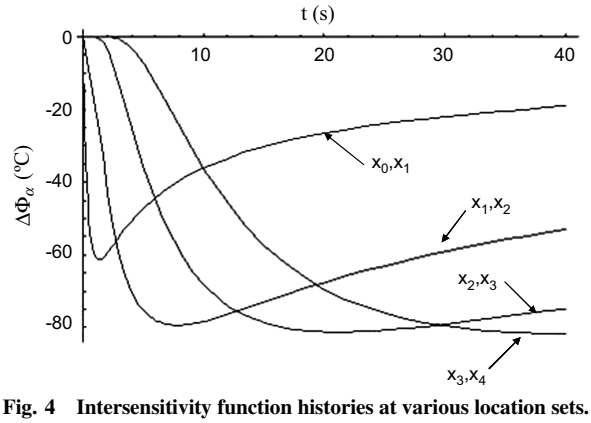

Fig. 4 Intersensitivity function histories at various location sets.

$$T_{\text{ref}} \triangleq \frac{q''_o x_2}{k\sqrt{\pi}} \tag{7b}$$

$$Fo_j \triangleq \frac{\alpha t}{x_j^2}, \qquad j = 1, 2 \tag{7c}$$

respectively, and where the probe distance ratio d is defined as

$$d = \frac{x_2}{x_1} \geq 1 \tag{7d}$$

Thus, the dimensionless modified intersensitivity function $\Delta\phi_\alpha$ can be plotted, as shown in Fig. 5, against the Fourier modulus associated with the deepest probe location x_2 as a function of probe distance ratio d. The maximum, absolute, dimensionless, modified intersensitivity is denoted as $\|\Delta\phi_\alpha\|_\infty$, while $Fo_{2,\infty}$ is the corresponding Fourier time where this maximum occurs. Figure 6 displays $\|\Delta\phi_\alpha\|_\infty$ against d, while Fig. 7 shows $Fo_{2,\infty}$ against d. From these figures, we see that $d = 2$ is approximately 60% of the rise and is representative of a nominal value since, as d grows beyond this value, relatively little gain in sensitivity is displayed.

This novel analysis is pertinent to experimental design since it provides guidance to sensor placement. For example, if $d = 2$, then $\|\Delta\phi_\alpha\|_\infty = 0.206$, from Fig. 6, while the corresponding Fourier number is $Fo_{2,\infty} \approx 0.2926$, as obtained from Fig. 7.

V. Thermal Diffusivity

In this section, we provide the basic derivation for arriving at the thermal diffusivity through the concept of rate-based sensing. To derive a third-order-accurate approximation for thermal diffusivity, we begin the process by recalling the Taylor series expansion about the point $x = x_2$ (per Fig. 1) as

$$T(x,t) = T(x_2,t) + \frac{\partial T}{\partial x}(x_2,t)(x-x_2) + \frac{\partial^2 T}{\partial x^2}(x_2,t)\frac{(x-x_2)^2}{2} + \frac{\partial^3 T}{\partial x^3}(x_2,t)\frac{(x-x_2)^3}{6} + \cdots \tag{8a}$$

$$q''(x,t) = q''(x_2,t) + \frac{\partial q''}{\partial x}(x_2,t)(x-x_2) + \frac{\partial^2 q''}{\partial x^2}(x_2,t)\frac{(x-x_2)^2}{2} + \frac{\partial^3 q''}{\partial x^3}(x_2,t)\frac{(x-x_2)^3}{6} + \cdots \tag{8b}$$

Fourier's law and one-dimensional energy conservation are given by

$$q''(x,t) = -k\frac{\partial T}{\partial x}(x,t) \tag{9a}$$

and

$$\rho C\frac{\partial T}{\partial t}(x,t) = -\frac{\partial q''}{\partial x}(x,t), \qquad (x,t) \geq 0 \tag{9b}$$

respectively. Upon eliminating q'' or T, we can obtain the heat equation in either temperature or flux as

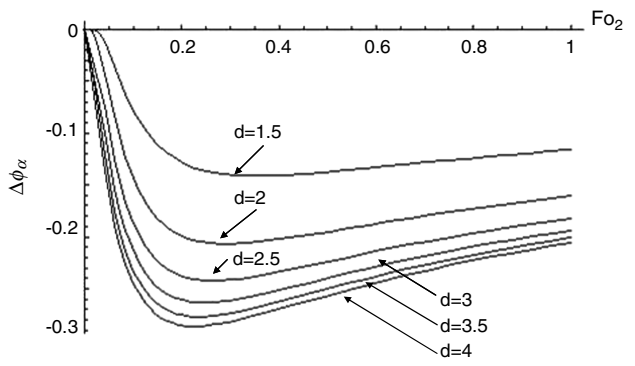

Fig. 5 Absolute dimensionless modified intersensitivity function as a function of the Fourier modulus for indicated values of d.

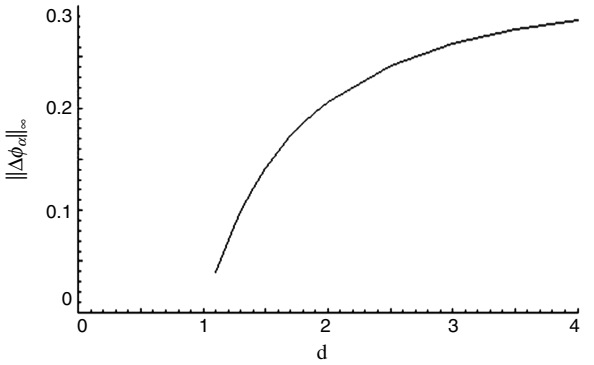

Fig. 6 The absolute maximum of dimensionless modified intersensitivity function as a function of the sensor depth ratio d.

$$\frac{1}{\alpha}\frac{\partial T}{\partial t}(x,t) = \frac{\partial^2 T}{\partial x^2}(x,t), \qquad (x,t) \geq 0 \tag{10a}$$

or

$$\frac{1}{\alpha}\frac{\partial q''}{\partial t}(x,t) = \frac{\partial^2 q''}{\partial x^2}(x,t), \qquad (x,t) \geq 0 \tag{10b}$$

respectively.

A third-order-accurate estimation for thermal diffusivity α is obtained by expressing all spatial derivatives given in the Taylor series [Eqs. (8a) and (8b)] in terms of temporal derivatives using Eqs. (9) and (10), removing all heat flux terms through Eq. (1b), evaluating x at x_1, and incorporating a series of analytical manipulations. After a lengthy but straightforward set of manipulations, we arrive at

$$\begin{aligned}
&\alpha^2 + \alpha\frac{(x_2-x_1)^2}{2[T(x_2,t)-T(x_1,t)]}\frac{\partial T}{\partial t}(x_2,t)\\
&\quad\times\left(1 - 2\left[\int_{u=0}^{t}\frac{\partial T}{\partial u}(x_2,u)\frac{\mathrm{d}u}{\sqrt{t-u}}\right]\right.\\
&\quad\left.\Big/\left\{\int_{u=0}^{t}\left[\frac{\partial T}{\partial u}(x_2,u) - \frac{\partial T}{\partial u}(x_1,u)\right]\frac{\mathrm{d}u}{\sqrt{t-u}}\right\}\right)\\
&\quad+\alpha^{1/2}\frac{(x_2-x_1)^3}{6\sqrt{\pi}[T(x_2,t)-T(x_1,t)]}\\
&\quad\times\int_{u=0}^{t}\frac{\partial^2 T}{\partial u^2}(x_2,u)\frac{\mathrm{d}u}{\sqrt{t-u}}\left(1 - 3\left[\int_{u=0}^{t}\frac{\partial T}{\partial u}(x_2,u)\frac{\mathrm{d}u}{\sqrt{t-u}}\right]\right.\\
&\quad\left.\Big/\left\{\int_{u=0}^{t}\left[\frac{\partial T}{\partial u}(x_2,u) - \frac{\partial T}{\partial u}(x_1,u)\right]\frac{\mathrm{d}u}{\sqrt{t-u}}\right\}\right)\\
&\quad-\frac{(x_2-x_1)^4}{6[T(x_2,t)-T(x_1,t)]}\frac{\partial^2 T}{\partial t^2}(x_2,t)\left(\left[\int_{u=0}^{t}\frac{\partial T}{\partial u}(x_2,u)\frac{\mathrm{d}u}{\sqrt{t-u}}\right]\right.\\
&\quad\left.\Big/\left\{\int_{u=0}^{t}\left[\frac{\partial T}{\partial u}(x_2,u) - \frac{\partial T}{\partial u}(x_1,u)\right]\frac{\mathrm{d}u}{\sqrt{t-u}}\right\}\right) = 0, \qquad t \geq 0
\end{aligned} \tag{11}$$

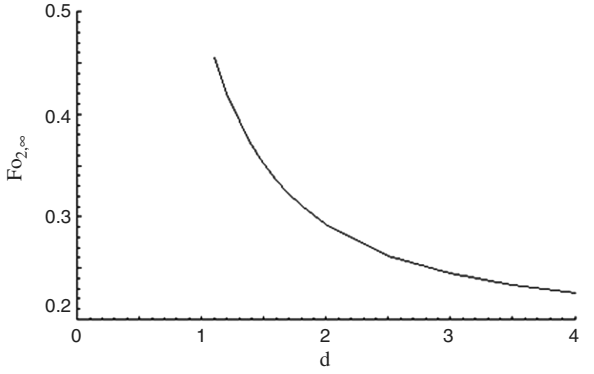

Fig. 7 The Fourier modulus at the maximum absolute intersensitivity as a function of the sensor depth ratio d.

Equation (11) is a fourth-degree polynomial equation in $\sqrt{\alpha}$. Equation (11) illustrates that the time rate of change of temperature sensors [13,14] (where $\partial T/\partial t \to \dot{T}$ and $\partial^2 T/\partial t^2 \to \ddot{T}$; i.e., analytic development to actual sensor) can be used to acquire the thermal diffusivity under constant property assumptions (small temperature changes). In a practical situation, the objective would involve developing the thermal diffusivity as a function of temperature. Thus, a series of tests would be required to cover the temperature range of interest. That is, a new initial condition can be established with the aid of an oven. thereby allowing the investigation to cover a large temperature range. The physics of diffusion is quite helpful, as high frequencies should be damped as penetration occurs. With this in mind, analog and/or digital filtering of data is strongly recommended.

VI. Results

This section presents a series of simulations illustrating the theoretical concepts described in Secs. IV and V. A dimensionally dependent variable is retained in this section for emulating experimental conditions. Consider the simple situation where a constant heat flux is imposed at $x = 0$, namely, $q''(0, t) = q''_0$ and $t > 0$ subject to the initial condition, $T(x, 0) = 0°\text{C}, x \in [0, \infty)$. The temperature distribution in the half space is given by Eq. (3b). As a specific example, let $q''_0 = 10^6$ W/m^2, $\alpha = 3.75 \times 10^{-6}$ m^2/s, $k = 14.7$ W/(m K), $x_1 = 5$ mm, and $x_2 = 10$ mm (hence, $d = 2$). This sensor placement permits a physically reasonable distance for the sensor installation process, since holes of a diameter less than 1 mm are possible. Recall that the resulting temperature histories are shown in Fig. 2. Figures 8 and 9 present the time histories for the first- and second-time derivatives of temperature from Eq. (3b) at the indicated locations. Observe that Eq. (11) does not require the second-time derivative of temperature at $x = x_1$.

Next, let us make use of the intersensitivity analysis to show that a single point in time (optimal) estimation of thermal diffusivity is theoretically possible under the idealized conditions. More important, these estimated values of thermal diffusivity and optimal time are used for guiding the degree of approximation mathematically developed in Sec. V. This will be shortly demonstrated.

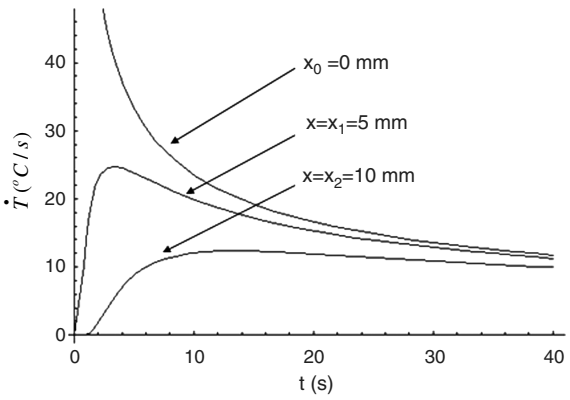

Fig. 8 Heating-rate histories at the indicated locations.

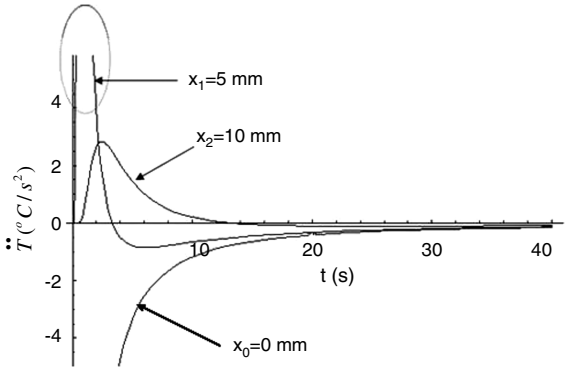

Fig. 9 Second-time derivative of temperature histories at the indicated locations.

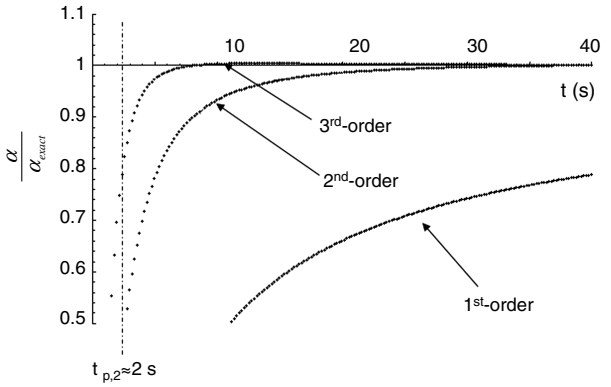

Fig. 10 Ratio of thermal diffusivities using different orders of truncation. A penetration time estimation is provided, illustrating that results before this time have no physical meaning.

Figure 10 demonstrates Eq. (11) as obtained using a rectangular integration rule and a Newton–Raphson procedure at each sample time step. Mathematica was used for all computations and graphics on a Dell Latitude D600. The first- and second-order methods (polynomials not given) are also displayed, showing that a third-order method is required in order to capture the time period where the maximum, absolute intersensitivity takes place, per Fig. 5. Figure 10 also illustrates both thermal penetration effects and truncation errors. Penetration time [16] (time for the thermal signal to be physically measured based on temperature at x_2) is estimated from $\alpha t_{p,2}/x_2^2 = 0.075$, which leads to $t_{p,2} \approx 2$ s. To further elaborate on the concept of penetration time, the classical integral method [16] can be used to solve the heat equation (in terms of temperature or heat flux) for a semi-infinite medium at a uniform initial temperature subject to a constant heat flux boundary at $x = 0$. If the heat flux is assumed to have a fourth-degree polynomial profile, the integral method solution for the dimensionless time required for the thermal front to reach a depth d is $Fo = 0.075$. Thus, for $t < 2$ s, the numerical results are meaningless. A third-order analysis is the best choice for the chosen values of d-based and x_2-based T, $\dot{T}$, and $\ddot{T}$ sensors. A second-order analysis requires the same set of sensors. A fifth-order analysis would require T, $\dot{T}$, $\ddot{T}$, and $\dddot{T}$ sensors. A fourth-order analysis would require the same set of sensors as the fifth-order analysis. Hence, odd orders of truncation are the most appropriate choices for implementation.

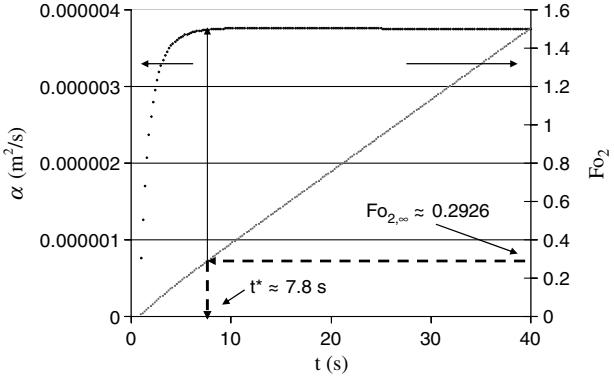

Fig. 11 Determination of the time t^* from $Fo_{2,\infty} = 0.2926$ when $\|\Delta\phi_\alpha\|_\infty = 0.206$ for $d = 2$. With this, a single-time evaluation at t^* for the thermal diffusivity, $\alpha^* = 3.743 \times 10^{-6}$ m^2/s (recall, $\alpha_{\text{exact}} = 3.75 \times 10^{-6}$ m^2/s) is attained. Observe, a slight curvature exists near $t^* = 7.8$ s on the α curve, indicating that truncation effects are still observable when $x_1 = 5$ mm and $x_2 = 10$ mm.

Figure 11 displays a two-vertical-axis plot illustrating how a single-time-point evaluation can be acquired for estimating the thermal diffusivity α^* when a sufficient α polynomial is chosen. The second vertical axis displays the Fourier modulus Fo_2. For $d = 2$, we previously determined the maximum, absolute intersensitivity value as $\|\Delta\phi_\alpha\|_\infty = 0.206$ (from Fig. 6) and subsequently determined the corresponding Fourier number as $Fo_{2,\infty} \approx 0.2926$ (from Fig. 7). With this, we next determine the time t^* at which this occurs. From Fig. 11, $t^* \approx 7.8$ s corresponds to the time of maximum intersensitivity for $d = 2$. Hence, we can estimate α by $\alpha^* = 3.743\times 10^{-6}$ m^2/s, which is 0.19% less than the exact value. Even with $x_1 = 5$ mm and $x_2 = 10$ mm, the third-order-accurate sensor approximation levels out near the maximum, absolute intersensitivity value.

Next, let us introduce measurement error into the simulated sensor data sets involving T, $\dot{T}$, and $\ddot{T}$ through

$$T_k = T(x_i, t_k) + \varepsilon_T \gamma_k \|T(x_i, t)\|_\infty, \quad i = 1, 2; \quad k = 1, 2, \ldots, M$$
$$\dot{T}_k = \dot{T}(x_i, t_k) + \varepsilon_{\dot{T}} \gamma_k \|\dot{T}(x_i, t)\|_\infty, \quad i = 1, 2; \quad k = 1, 2, \ldots, M$$
$$\ddot{T}_k = \ddot{T}(x_i, t_k) + \varepsilon_{\ddot{T}} \gamma_k \|\ddot{T}(x_i, t)\|_\infty, \quad i = 1, 2; \quad k = 1, 2, \ldots, M \quad (12)$$

where $\varepsilon_T = 0.005$, $\varepsilon_{\dot{T}} = 0.02$, $\varepsilon_{\ddot{T}} = 0.04$, and $\gamma_k =$ random number $\in [-1, 1]$.

Figures 12–14 present numerically simulated data for 1) the temperature, 2) the heating rate, and 3) the second-time derivative of temperature, where $M = 200$. Figure 15 indicates that the optimal time for a single-point estimation of the thermal diffusivity occurs near $t^* \approx 7.88$ s and attains the value of $\alpha^* \approx 3.71 \times 10^{-6}$ m^2/s, which is a highly favorable result (1.07% less than the exact value) in light of the ideal (exact) thermal diffusivity of $\alpha_{\text{exact}} = 3.75\times 10^{-6}$ m^2/s. It may be noted that the average predicted thermal diffusivity in the time span $t \in [10, 40]$ s in Fig. 15 is 3.81×10^{-6} m^2/s, which is 1.6% more than the exact value.

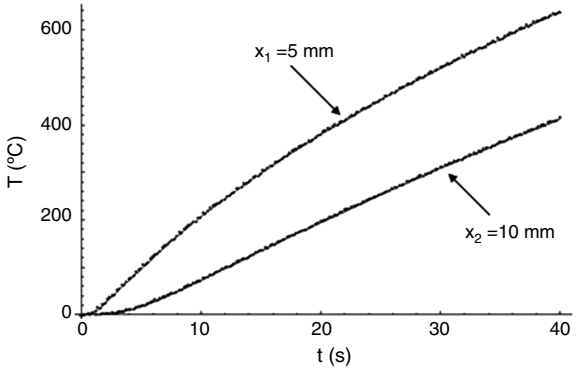

Fig. 12 Exact (lines) and noisy (solid circles) simulated data, Eq. (12), for the temperature at the two indicated locations.

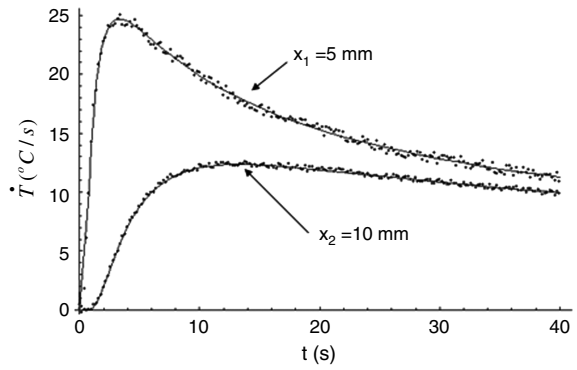

Fig. 13 Exact (lines) and noisy (solid circles) simulated data, Eq. (12), for the heating rate at the two indicated locations.

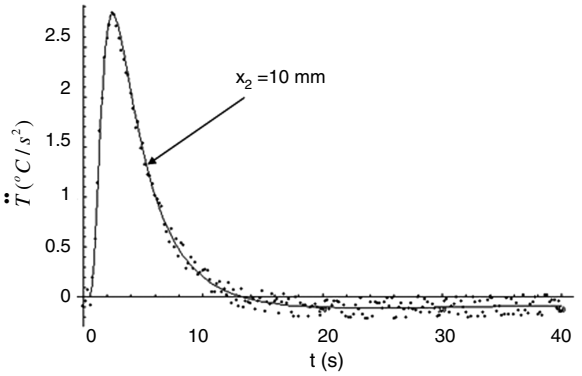

Fig. 14 Exact (lines) and noisy (solid circles) simulated data, Eq. (12), for the second time derivative of temperature at the indicated location.

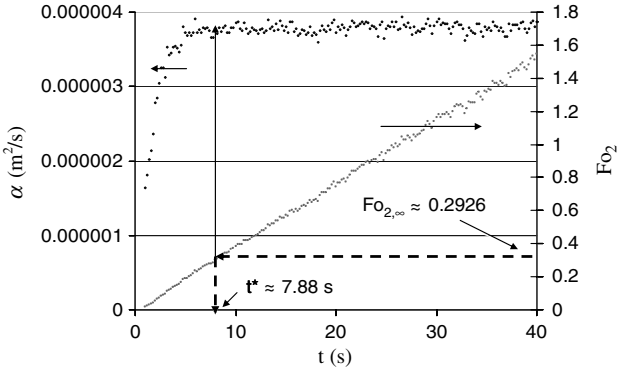

Fig. 15 Estimating thermal diffusivity α^* under noisy conditions at the maximum intersensitivity. Here, $\alpha^* = 3.71 \times 10^{-6}$ m^2/s at time $t^* \approx 7.88$ s (calculated based on linear interpolation between data points and $Fo_{2,\infty}$).

VII. Conclusions

The proposed in situ approach for estimating thermal diffusivity has been theoretically considered, and a novel intersensitivity analysis has been proposed. Based on the preliminary numerical results, this approach represents a new methodology for estimating thermal diffusivity based on a time-domain view of heat flux. In a practical situation, the objective would involve developing the thermal diffusivity as a function of temperature. Thus, a series of tests would be required to cover the temperature range of interest. That is, a new initial condition can be established with the aid of an oven, thereby allowing the investigation to cover a large temperature range. Our future work will include developing an experimental facility for validating the proposed analysis.

References

[1] Frankel, J. I., "Regularization of Inverse Heat Conduction by Combination of Rate Sensors Analysis and Analytic Continuation," *Journal of Engineering Mathematics*, Vol. 57, No. 2, 2007, pp. 181–198.
doi:10.1007/s10665-006-9073-y

[2] Frankel, J. I., Keyhani, M., Arimilli, R. V., and Wu, J., "A New Multidimensional Integral Relationship Between Heat Flux and Temperature for Direct Internal Assessment of Heat Flux," *Zeitschrift für Angewandte Mathematik und Physik*, Vol. 59, No. 5, 2008, pp. 869–888.
doi:10.1007/s00033-007-6135-6

[3] Frankel, J. I., Keyhani, M., and Arimilli, R. V., "A New, Orthotropic, Two-Dimensional, Transient Heat Flux-Temperature Integral Relationship for Half-Space Diffusion," *Journal of Thermophysics and Heat Transfer*, Vol. 24, No. 1, 2010, pp. 212–215.
doi:10.2514/1.43265

[4] Frankel, J. I., Keyhani, M., Arimilli, R. V., and Elkins, B., "A New, Anisotropic, Two-Dimensional, Transient Heat Flux-Temperature

Integral Relationship for Half-Space Diffusion," *Zeitschrift für Angewandte Mathematik und Mechanik (ZAMM)*, Vol. 90, No. 2, 2010, pp. 161–170. doi:10.1002/zamm.200900326

[5] Diller, T. E., "Advances in Heat Flux Measurements," *Advances in Heat Transfer*, Vol. 23, Academic Press, New York, 1993, pp. 279–368.

[6] Lu, F. K., and. Kinnear, K. M., "Characterization of Thin Film Heat Flux Gauges," 20th Advanced Measurement and Ground Testing Technology Conference, AIAA Paper 1998-2504, June 1988.

[7] Cook, W. J., and Felderman, E. J., "Reduction of Data from Thin-Film Heat Transfer Gages: A Concise Numerical Technique," *AIAA Journal*, Vol. 4, No. 3, 1996, pp. 561–562. doi: 10.2514/3.3486

[8] Kress, R., *Linear Integral Equations*, Springer–Verlag, Berlin, 1989.

[9] Frankel, J. I., and Arimilli, R. V., "Inferring Convective and Radiative Heating Loads from Transient Surface Temperature Measurements in the Half-Space," *Inverse Problems in Sciences and Engineering*, Vol. 15, No. 5, 2007, pp. 463–488. doi:10.1080/17415970600795378

[10] Hanke, M., and Scherzer, O., "Inverse Problems Light: Numerical Differentiation," *American Mathematical Monthly*, Vol. 108, No. 6, 2001, pp. 512–520. doi:10.2307/2695705

[11] Groetsch, T., "Differentiation of Approximately Specified Functions," *American Mathematical Monthly*, Vol. 98, No. 9, 1991, pp. 847–850. doi:10.2307/2324275

[12] Frankel, J. I., Arimilli, R. V., Keyhani, M., and Wu, J., "Heating Rate dT/dt Measurements Developed from In Situ Thermocouples using a Voltage-Rate Interface," *International Communications in Heat and Mass Transfer*, Vol. 35, No. 8, 2008, pp. 885–891. doi:10.1016/j.icheatmasstransfer.2008.04.019

[13] Elkins, B., Huang, M. G., and Frankel, J. I., "Higher-Time Derivative of Temperature Sensors for Aerospace Heat Transfer," 41st AIAA Thermophysics Conference, AIAA Paper 2009-4236, June 2009.

[14] Kruttiventi, J., Wu, J., and Frankel, J. I., "Real-Time Low-Noise Differentiation of Low Frequency Signals in Heat-Transfer Applications," *IEEE Transactions on Instrumentation and Measurement*, Vol. 59, No. 3, 2010, pp. 596–603. doi:10.1109/TIM.2009.2025069

[15] Dowding, K. J., Blackwell, B. F., and Cochran, R. J., "Application of Sensitivity Coefficients for Heat Conduction Problems," *Numerical Heat Transfer, Part B: Fundamentals*, Vol. 36, No. 1, 1999, pp. 33–55. doi:10.1080/104077999275767

[16] Ozisik, M. N., *Heat Conduction*, Wiley, New York, 1980, pp. 335–340.